

Identification of rigosertib for the treatment of recessive dystrophic epidermolysis bullosa-associated squamous cell carcinoma

Velina S. Atanasova^{1*}, Celine Pourreyn^{2*}, Mehdi Farshchian¹, Christian A. Brown IV¹, Stephen A. Watt², Sheila Wright², Michael Warkala¹, Christina Guttman-Gruber³, Josefina Piñón Hofbauer³, Ignacia Fuentes^{4,5}, Marco Prisco¹, Elham Rashidghamat⁶, Cristina Has⁷, Francis Palisson^{4,8}, Alain Hovnanian⁹, John A. McGrath⁶, Jemima E. Mellerio⁶, Johann Bauer³, Andrew P. South^{1*}.

¹Department of Dermatology and Cutaneous Biology, Thomas Jefferson University, Philadelphia, PA

²Division of Cancer Research, University of Dundee, Dundee, UK

³EB House Austria, Research Program for Molecular Therapy of Genodermatoses, Department of Dermatology, University Hospital Salzburg, Paracelsus Medical University Salzburg, Austria

⁴Fundación DEBRA Chile, Santiago, Chile

⁵Centro de Genética y Genómica, Facultad de Medicina Clínica Alemana, Universidad del Desarrollo, Santiago, Chile

⁶St. John's Institute of Dermatology, King's College London (Guy's Campus), London, UK

⁷ Department of Dermatology, Medical Center – University of Freiburg, Freiburg, Germany

⁸Facultad de Medicina Clínica Alemana, Universidad del Desarrollo, Santiago, Chile

⁹INSERM UMR 1163, Paris, France; Imagine Institute, Paris, France

Running title: Rigosertib for RDEB SCC therapy

Keywords (5): squamous cell carcinoma, recessive dystrophic epidermolysis bullosa, PLK1, RAS, CRAF, AKT

Financial support: This work was supported by DEBRA International – funded by DEBRA UK (grant to APS, and grant to APS, JB, JEM)

* *Correspondence:* Dr Andrew P South, Dermatology and Cutaneous Biology, Thomas Jefferson University, 233 S. 10th Street, BLSB 406, Philadelphia, PA. Tel: (215) 955 1934; Fax: (215) 503 5774. E-mail: Andrew.south@Jefferson.edu.

† These authors contributed equally to this work.

The authors state no conflict of interests.

Word count: XX

Number of figures and tables: 6

Statement of translational relevance (150 word)

Collectively our data support a clinical trial of rigosertib for treatment of recessive dystrophic epidermolysis bullosa-associated squamous cell carcinoma, an inherently aggressive sub-type of squamous cell carcinoma with extremely low 5-year survival. Currently there are no effective treatments for this devastating cancer and often times initial SCC will recur and readily metastasize; any effective systemic therapy that reduces the tumor burden will improve quality of life in this patient population.

Abstract

Squamous cell carcinoma (SCC) of the skin is the leading cause of death in patients with the severe generalized form of the genetic disease recessive dystrophic epidermolysis bullosa (RDEB). Although emerging data are identifying why patients suffer this fatal complication, therapies for treatment of RDEB SCC are in urgent need. We previously identified polo-like kinase 1 (PLK1) as a therapeutic target in skin SCC, including RDEB SCC. Here, we present a screen of 6 PLK1 inhibitors and identify a lead compound, ON-01910 (or rigosertib), that exhibits significant specificity for RDEB SCC: in culture rigosertib induced apoptosis in 10/10 RDEB SCC keratinocyte populations while only affecting normal primary skin cells at doses 2-4 orders of magnitude higher. Furthermore, rigosertib significantly inhibited the growth of two RDEB SCC in murine xenograft studies and showed no apparent toxicity. Mechanistically rigosertib has been shown to inhibit PLK1 indirectly by targeting RAS-effector signaling pathways. In agreement with these observations rigosertib inhibited phosphorylation of CRAF in SCC keratinocytes in culture with less of an effect to non-SCC primary keratinocytes. In addition, rigosertib selectively reduced phosphorylated AKT levels in RDEB SCC keratinocytes with little effect to non-SCC primary keratinocytes suggesting that specificity of rigosertib for SCC may be linked to this pathway. Our data support a "first in RDEB" phase I/II clinical trial of rigosertib to assess tumor targeting in patients with late stage, metastatic and/ or unresectable SCC.

Introduction

Patients with the devastating inherited skin disease recessive dystrophic epidermolysis bullosa (RDEB) are at significantly increased risk of developing aggressive cutaneous squamous cell carcinoma (SCC), which is the cause of death by age 45 years in 70% of individuals with the severe generalized form of the disease(1, 2). Furthermore, 5 year survival in all RDEB sub-types diagnosed with SCC is close to 0% (2) making RDEB SCC one of the most aggressive forms of this tumor type. Current clinical guidelines offer limited options for RDEB SCC and consist of wide local excision, radiotherapy, and in late stages, limb amputation (3). New approaches to therapy for RDEB SCC are in urgent need.

RDEB is caused by mutations in *COL7A1*, the gene encoding type VII collagen (4). However, *COL7A1* does not behave as a classical tumor suppressor as heterozygous carriers are not at increased risk of skin cancer and *COL7A1* has not been identified as a significantly mutated gene in genetic profiling of any tumor type to date. RDEB is characterized by skin fragility, trauma induced skin blistering, and chronic non-healing wounds (5) and work by us and others has implicated the tumor microenvironment as a driving mechanism of cancer development (6, 7). Our recent comprehensive genetic characterization demonstrates that RDEB SCC are driven by somatic mutation in driver genes that are identical to UV-induced skin SCC and head and neck SCC (HNSCC) (8) and we have **been consistently been** unable to identify genetic mechanisms which explain the aggressive nature of RDEB SCC (9, 10). Our early microarray gene expression profiling failed to significantly differentiate RDEB from skin SCC in cultured keratinocytes (10). However, this work did identify polo-like kinase 1 (PLK1) as a therapeutic target in RDEB SCC.

Here we follow up this finding with a screen of available PLK1 inhibitors and identify ON-01910, or rigosertib, as a lead candidate for therapy in RDEB SCC.

Materials and Methods

Cell cultures

Cells were isolated from biopsies taken as part of routine surgical or diagnostic procedures. Informed written consent was obtained from each patient or in the case of under-aged children from their parents or guardian. This study was performed in accordance with the Helsinki declaration. All cells were isolated as described (11) and cultured at 37° C in 5% CO₂. Keratinocytes were grown in Dulbecco's modified essential medium (DMEM, Corning cellgro, Mediatech Inc, Manassas, VA)/ Ham's F12 medium (3:1), supplemented with 10% fetal bovine serum (FBS, PEAK Serum, Cat PS-FB1, Colorado, USA), 10 ng/ml of epidermal growth factor, 10⁻¹⁰ M cholera toxin, 0.4 µg/ml of hydrocortisone, 5 µg/ml of transferrin, 5 µg/ml of insulin and 5 µg/ml liothyronine.

Protein Quantification

Total lysates were quantified using Pierce bicinchoninic assay Protein Assay kit (Fisher Scientific, Waltham, MA) and 5-50 µg of protein were loaded onto SDS-PAGE gel. The signal from Western blot analysis was quantified with Image J. P-CRAF and P-AKT were quantified relative to GAPDH.

Drug treatment and western blot analysis

Rigosertib (ON 01910.Na) was either purchased from Selleckchem.com (Houston, TX) or provided by Onconova Therapeutics, Inc. (Newtown, PA). 2-4 x 10⁵ Keratinocytes were plated in a 6 well dish. On the following day, the medium was changed with the drug at 1 µM or vehicle control. Medium was left for 48 hours and cells were lysed with radioimmunoprecipitation

assay buffer. Lysate was placed in a centrifuge for 5 minutes at 4°C, and the supernatant was mixed with a 6x Laemmli loading buffer. Samples were boiled for 5 minutes at 95°C before being loaded onto SDS-PAGE gels. Primary antibodies used were: PLK1 (Cell Signaling, 208G4), CRAF polyclonal (Cell signaling, 9422S), P-CRAF (Cell signaling, 9427S), P-AKT (Cell signaling, 9271), AKT (Cell signaling, 9272), GAPDH (Santa Cruz, 6C5). Resolved proteins were transferred onto nitrocellulose membrane with a BioRad Trans-Blot-Turbo (Bio-Rad, Hercules, CA), blocked in PBS-0.1% Tween with 5% milk or 5% BSA according to requirements of the primary antibody, and incubated overnight with the primary antibody. After incubation with IgG-HRP conjugated secondary antibody (Santa Cruz Biotechnology), membrane was incubated with Pierce ECL Western blotting substrate (Fisher Scientific, Waltham, MA) and exposed to CL-XPosure X-ray film (Fisher Scientific, Waltham, MA).

Immunofluorescence

RDEB SCC and human control skin biopsies were frozen in optimal cutting temperature (OCT, Sakura Finetek USA, Torrance, CA) and cut at 6 microns on a cryostat. Sections were fixed with 50:50 methanol: acetone mixture for 5 minutes. Slides were rinsed with 1x PBS, permeabilized with PBS/0.1% Tween 20 (Sigma Aldrich, St. Louis, MO) for 5 minutes followed by blocking for 1 hour with PBST/3% BSA (Sigma Aldrich, St. Louis, MO). Primary antibodies were incubated for 1.5 hours at room temperature. Secondary antibody Alexa Fluor 594 goat anti-rabbit (1:800, Molecular Probes Eugene, OR) were applied for 1 hour at room temperature. Slides were cover-slipped with hard set 4,6-diamidino-2-phenylindole (DAPI; Vector Labs, Burlingame, CA) and examined by fluorescence microscopy (EVOS FL cell imaging system, ThermoFisher).

MTS assay

Colorimetric assays of mitochondrial dehydrogenase activity were performed using the MTS CellTitre 96 AQueous One Solution Cell Proliferation Assay (Promega, Madison, WI, USA) according to the manufacturer's instructions. In each case cells were seeded into replica 96-well plates and readings were taken at intervals up to a maximum of 96 h. We have previously shown that an increase in mitochondrial dehydrogenase activity using this assay directly correlates with primary non-SCC and SCC cell number determined using a CASY Model TT cell counter (Roche Diagnostics Ltd, West Sussex, UK) (10).

Cell Cycle analysis

5-Bromodeoxyuridine (BrdU; Sigma-Aldrich) was added at 30 mM final concentration for 20 min. Cells were collected and fixed by dropping a 1-ml cell suspension in phosphate-buffered saline into 3ml ice-cold ethanol while vortexing. Pepsin (Sigma) was added at 1 mg/ml in 30mM HCL for 30 min and DNA was denatured with 2N HCL for 20 min. An anti-BrdU antibody diluted in phosphate-buffered saline/0.5% Tween/ 0.5% bovine serum albumin was added for 1 h followed by 30-min incubation with a fluorescein isothiocyanate-sheep anti-mouse IgG (Sigma). Propidium iodide (Sigma) was added in the final wash step at a concentration of 25 mg/ml and samples were analyzed using a FACScan flow cytometer and the CellQuest software (Becton Dickinson).

Apoptosis ELISA

Apoptosis was measured using the Cell Death Detection ELISA^{PLUS} (ROCHE, cat# 11774425001). Briefly, non-SCC keratinocytes were plated at 5×10^3 cells /well and SCC keratinocytes at 2.5×10^4 cells /well in 96 well plates. On the next day the cells were treated with the drug (1 μ M) for 16 to 24 hours. Cells were lysed for 30 minutes and 20 μ l of the lysate was incubated with 80 μ l immunoreagent. After incubation the reaction was stopped with ABTS solution and absorbance was read using a plate reader at 405 nm and 490 nm.

In vivo tumor growth and treatment

All animal experiments were conducted in accordance with UK Home Office and Thomas Jefferson IACUC regulations. For tumorigenicity assays a suspension of $1-2 \times 10^6$ tumor cells was mixed with high-concentration Matrigel (Becton Dickinson, Oxford, UK) and injected subcutaneously into the flanks of SCID Balb/c mice. Tumors were measured by a caliper and treatment began when volume reached 100-200mm³. Animals were treated with 20mg/kg rigosertib dissolved in PBS.

Results

PLK1 is increased in RDEB SCC

We previously identified PLK1 mRNA was increased in 4 RDEB SCC keratinocyte cultures compared with normal primary keratinocyte controls (10). Here we extend this observations to a total of 10 separate SCC populations and identify PLK1 increased in 10 of 10 fresh frozen RDEB SCC tissue samples using immuno-histochemistry (**Figure 1**).

ON-01910 emerges with the largest delta comparing growth in RDEB SCC and primary skin cells

After confirmation of increased PLK1 in all RDEB SCC assessed we set out to compare the efficacy of commercially available PLK1 inhibitors for targeting RDEB SCC. We initially assessed the effects of 6 PLK1 inhibitors on cell metabolism using an MTS assay after 48 hours exposure to normal primary keratinocytes, RDEB primary fibroblasts (n=4), RDEB SCC keratinocytes (n=4) and UV-induced, non-RDEB SCC keratinocytes (**Table 1**). These data identified the compound ON-01910, also known as rigosertib, as having the greatest specificity for RDEB SCC keratinocytes when compared with normal primary keratinocytes and RDEB primary fibroblasts (**Table 1**). In this set of experiments rigosertib showed up to 4 orders of magnitude specificity for reducing RDEB SCC cell metabolism compared with primary non-RDEB keratinocytes or fibroblasts isolated from RDEB skin or RDEB SCC.

Next, these data were confirmed in a further 7 separate patient derived RDEB SCC cell lines (bringing the total to 11) using crystal violet uptake by live cells after 48 hours exposure to varying drug concentrations (**Figure 2A** and **B**). We also observed that whereas higher concentrations of rigosertib inhibited the growth of non-SCC primary keratinocytes in culture

(both RDEB and non-RDEB, **Figure 2A** and **B**) no obvious signs of cell death were evident while in RDEB SCC keratinocyte populations cell death was widespread (**Figure 2C**).

ON-01910 induces apoptosis in RDEB SCC keratinocytes

In agreement with our previous data using PLK1 siRNA and the PLK1 inhibitors BI-2536 and GW-843682 (10), as well as published studies of rigosertib (12-14), exposure of RDEB SCC keratinocytes to rigosertib induced cell cycle arrest and apoptosis in RDEB SCC keratinocytes (**Figure 3A-B**).

ON-01910 reduces phosphorylation of AKT and CRAF in RDEB SCC keratinocytes

Since its identification as an inhibitor of PLK1, rigosertib has been shown to inhibit a variety of kinases, including AKT (12). Most recently rigosertib has been shown to compete with activated RAS for binding to CRAF (15). In agreement with these studies rigosertib inhibited phosphorylation of both AKT and CRAF in RDEB SCC keratinocytes (**Figure 3C**).

ON-01910 effectively targets RDEB SCC keratinocytes in vivo

Next we sought to establish the ability of rigosertib to target RDEB SCC keratinocytes in vivo. Tumor xenograft models showed that either local tumor injection (**Figure S1**) or systemic delivery (**Figure 4**) effectively inhibited the growth of two separate RDEB SCC keratinocyte cell lines in vivo. Ki-67 immuno-histochemistry showed that tumors harvested from those animals treated with rigosertib had significantly fewer proliferative tumor cells than vehicle control treated animals (**Figure 4D** and **E**).

Discussion

SCC is a lethal complication for the majority of patients with the already devastating genetic disease RDEB and currently there are no approved or effective therapies for SCC in this patient population (3). Here we present evidence that the multi-kinase inhibitor rigosertib effectively induces apoptosis or targets in vivo tumor growth in 11/11 separate RDEB SCC populations, data which support a clinical trial of rigosertib in RDEB SCC. In particular, the lack of significant targeting of non-tumor cells by rigosertib (**Figure 2**), the lack of any observed toxicity in our animal studies coupled with the overall favorable side-effect profile for this drug as determined by trials in patients with myelodysplastic syndrome (16) supports the notion that even in a patient group such as RDEB, where numerous clinical complications abound as a result of lack of mechanical integrity of the epidermis, rigosertib may be well tolerated.

Previous studies of rigosertib in the context of head and neck SCC (HNSCC) have demonstrated similar efficacy in a sub-set of tumor cell lines/ populations (17). The data presented in our study shows remarkable sensitivity of RDEB SCC to rigosertib and suggests that this subtype of SCC may respond to rigosertib treatment more favorably. The mechanism of such specific sensitivity remains unknown and understanding this may offer precision medicine opportunities for use of rigosertib in subsets of sporadic SCC arising at different anatomical locations. We have recently increased our current understanding of RDEB SCC through comprehensive genomic characterization of 27 tumors which shows that other than mutation burden and mechanism, the somatic mutation profile in RDEB SCC is no different to HNSCC or UV induced skin SCC, and that RDEB SCC are most similar to the basal and mesenchymal sub-types of

HNSCC at the level of transcriptomics (8). This similarity to sub-types of HNSCC at the level of mRNA expression may begin to offer opportunity for identifying biomarkers of drug sensitivity and we are actively pursuing this line of inquiry. Another feature identified in RDEB SCC is homogeneity at the level of somatic tumor driver-gene mutation (8) and this may be advantageous in the context of targeted therapies where often resistance that develops is often associated with genetic heterogeneity (18).

Finally, rigosertib reduced phosphorylation of both CRAF and AKT in cultured RDEB SCC keratinocytes with the greatest and consistent reduction in AKT (**Figure 3C**). These observations may point to a mechanistic link between RAF activation and PI3K pathway activation that is specific to RDEB SCC and future work will concentrate on understanding this relationship with apoptosis induction in RDEB SCC.

Acknowledgements

This work was supported by DEBRA International – funded by DEBRA UK (grants to APS, and to APS, JB, JEM). We would like to thank all the patients who contributed to this study as well as Evan Greenawalt for technical assistance.

Tables

Table 1: EC₅₀ values as determined by MTS assay for primary non-SCC and SCC keratinocytes and primary fibroblasts. NT = not tested. Sensitivity RDEB SCC vs Normal Cells calculated by dividing the average EC₅₀ value for non-tumor keratinocytes by the average EC₅₀ value for RDEB SCC keratinocytes.

Cell Type	ID	BI2536	BI6727	GSK46136 4	GW84368 2	HMN214	ON-01910
Primary normal keratinocytes	NHK	1.52	2.04	9.15	N/T	9.45	310.59
Primary EB fibroblasts	RDEB27F	6.21	5.97	12.90	849.82	65.16	34135.27
Primary EB SCC fibroblasts	RDEB1SCCF	5.99	3.80	5.09	103.41	4.40	11.01
Primary EB SCC fibroblasts	RDEB5SCCF	4.32	2.61	8.73	124.44	5.30	247.26
Primary EB SCC fibroblasts	RDEB58SCCF	4.78	3.69	13.03	103.17	13.46	110.49
SCCRDEB	SCCRDEB2K	0.34	N/T	0.14	0.14	0.30	0.06
SCCRDEB	SCCRDEB3K	1.57	0.44	3.87	0.45	0.17	0.14
SCCRDEB	SCCRDEB4K	0.99	1.78	1.88	98.27	0.27	0.10
SCCRDEB	SCCRDEB16K	0.75	0.57	13.80	1.34	0.53	0.27
SCC	SCCIC1	1.15	2.45	12.10	N/T	0.70	0.10
Sensitivity RDEB SCC vs Normal Cells		4.76	2.77	1.54	11.78	49.88	52739.04

Table 2: Cells used in this study. N/A = not available. Column 2 indicates the tumor # from recent characterization of somatic mutations in the given cell population or from the tumor which the cells were derived (8).

Sample	Tumor # Cho et al.	COL7A1 Genotype	Body Site	Primary/recurrence	Age	Sex
SCCRDEB2	RDEBSCC_02	c.6269delC (p.P2090LfsX116) / c.8253_8254delAG (p.R2751SfsX38)	Forearm	Primary	54	Male
SCCRDEB3	RDEBSCC_03	c.1573C>T (p.R525X) / c.1732C>T (p.R578X)	L. Forearm	Primary	35	Female
SCCRDEB4	N/A	c.8244insC/ c.8244insC	Shoulder	Primary	32	Female
SCCRDEB16	RDEBSCC_26	c.2470dupG (p.N825KfsX41) / c.3948insT (p.G1317WfsX43)	Foot	Primary	28	Female
SCCRDEB53	RDEBSCC_09	c.682+1G>A / c.3809C>T (p.P1270L)	R. Forearm	Primary	28	Female
SCCRDEB62	RDEBSCC_11	c.2005C>T (p.R669X) / c.2005C>T (p.R669X)	L. Elbow	Primary	31	Female
SCCRDEB70	RDEBSCC_27	c.425A>G (p.K142R) / c.425A>G (p.K142R)	L. Elbow	Metastasis	27	Male
SCCRDEB71	RDEBSCC_28	c.IVS34-1G>A; / c.3840delC (p.G1281VfsX44)	L. Hand	Recurrence	35	Female
SCCRDEB99	RDEBSCC_29	c.6527dupC (p.G2177WfsX113) / c.5532+1G>T	Back	Primary	24	Male
SCCRDEB106	RDEBSCC_30	c.5532+1G>T / c.3264_5293del (p.Q1089_G1764fsX7)	Back	Primary	50	Male
SCCRDEB108	RDEBSCC_31	c.4894C>T (p.R1632X) / c.8440C>T (p.R2814X)	L. Knee	Primary	23	Female
RDEB1	N/A	c.1732C>T (p.R578X) / c.7786delG (p.G2596VfsX35)	Hand	-	37	Male
RDEB5	N/A	c.1732C>T (p.R578X) / (p.Q905X)	N/A	-	29	Female
RDEB27	N/A	c.2470dupG (p.N825KfsX41) / c.2470dupG (p.N825KfsX41)	Arm	-	N/A	Female
RDEB58	N/A	N/A	N/A	-	N/A	N/A
RDEB81	N/A	c.2923_2924insA / p.A975fs / not found	Arm	-	29	Female
RDEB84	N/A	c.8697del11 (p.S2900Lfs*20) / c.8697del11 (p.S2900Lfs*20)	Arm	-	2	Male
RDEB85	N/A	c.6101G>C (p.G2034A) / c.2044C>T (p.R682X)	Arm	-	11	Male
RDEB86	N/A	N/A	Arm	-	3	Female
RDEB93	N/A	c.5051_5052insGAAA (p.N1684fs) / c.2471dupG (p.G824fs)	Arm	-	35	Male
RDEB115	N/A	c.4249delG / (p.R1933X)				

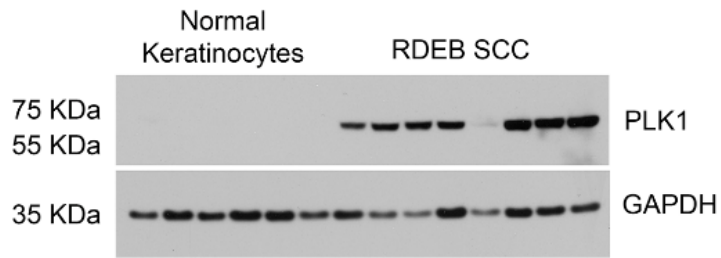
RDEB118	N/A	c.1732C>T in exon 13 p.Arg578* / c.7474C>T in exon 98 p.Arg2492*	Heel	-	37	Female
RDEB124	N/A					
FS1	N/A	Normal Foreskin Sample, N/A	Foreskin	-	0	Male
Br43,46,61,63	N/A	Normal Breast Samples, N/A	Breast	-	33,23,20 and 31	Female

Figures

Figure 1: PLK1 is increased in RDEB SCC

A: 5ug of total cell lysate was resolved on a 6% SDS PAGE gel, transferred to nitrocellulose membrane before being incubated with antibodies raised against PLK1 (Cell Signaling, 208G4) and GAPDH (Santa Cruz, 6C5). Samples loaded from left to right: lanes 1-2 = normal primary breast keratinocytes (Br61, Br63), lanes 3-6 = RDEB primary keratinocytes (RDEB81, RDEB84, RDEB85, RDEB118), lanes 7-14 = RDEB SCC keratinocytes (SCCRDEB108, SCCRDEB2, SCCRDEB3, SCCRDEB70, SCCRDEB71, SCCRDEB4, SCCRDEB62, SCCRDEB106). **B:** 6uM frozen sections were processed and incubated with an antibody raised against PLK1 (Sigma-Aldrich, HPA053229) (red) as well as the nuclear stain DAPI (blue). Bar = 400uM.

A



B

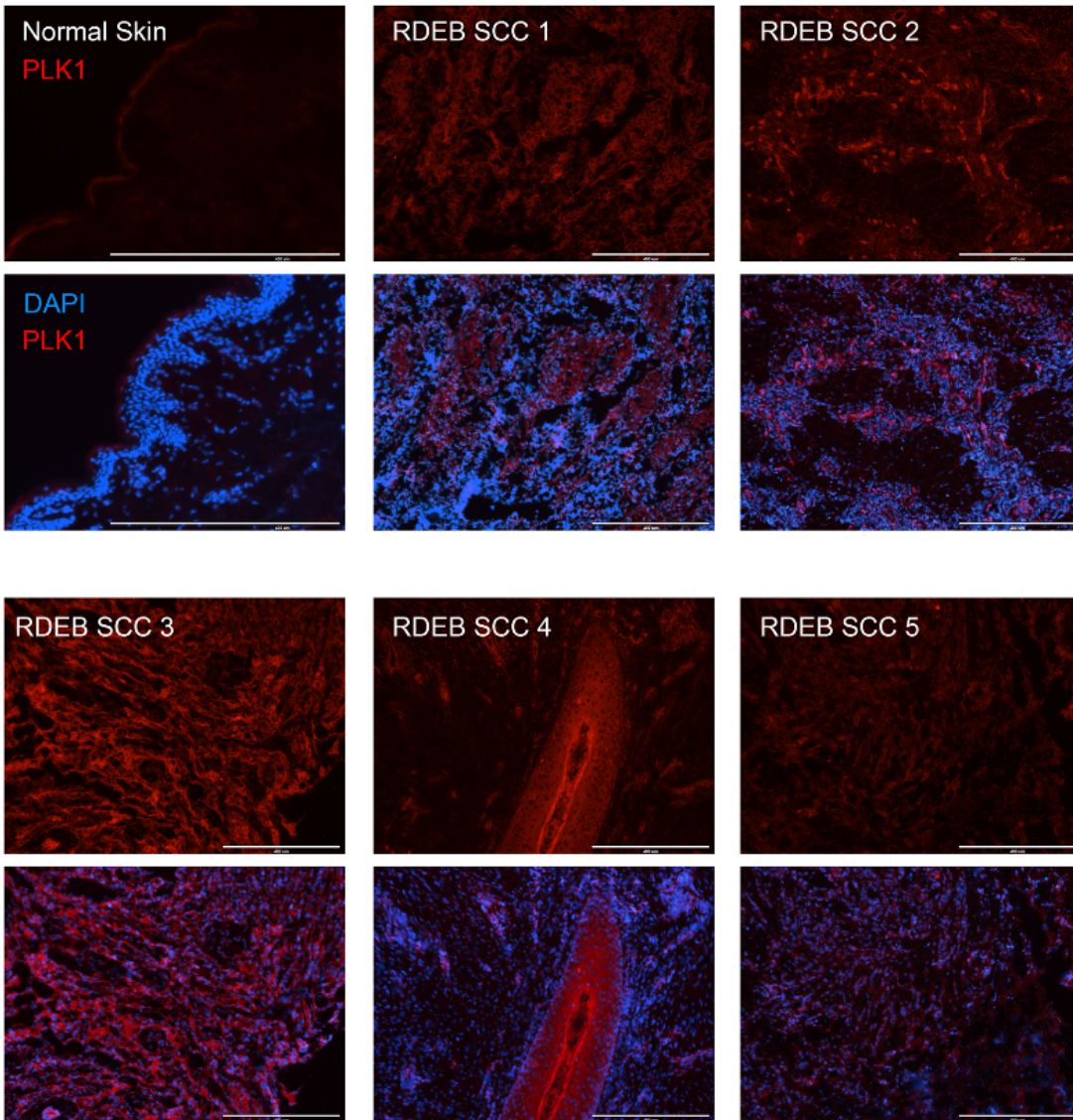


Figure 2: Rigosertib effectively targets RDEB SCC keratinocytes in vitro

A: Normal primary keratinocytes (FS1, Br61), RDEB primary keratinocytes (RDEB81, RDEB84), and RDEB SCC keratinocytes (SCCRDEB2, SCCRDEB3, SCCRDEB4) were seeded into wells of a 96 well plate and exposed to vehicle (DMSO) or increasing concentrations of rigosertib (0.01-100uM) for 48 hrs. Cells were then fixed with 70% ETOH and incubated with the cell dye crystal violet. Plate was photographed after excess dye was washed away with water. **B:** Crystal violet retention was measured using a spectrometer and values relative to vehicle alone were calculated for cells exposed to increasing concentrations of rigosertib. Graph shows average change from control (+/- SD) from a single experiment using 2 populations of normal primary keratinocytes (Br61, Br63), 2 population of primary RDEB keratinocytes (RDEB81, RDEB84) and 10 populations of RDEB SCC keratinocytes (see **Table 1**). **C:** Cells were plated into a 6-well plate and incubated with vehicle alone or 1uM of rigosertib for 48 hrs before photographs were taken. Br63 (Primary normal) and SCCRDEB3 cells were used.

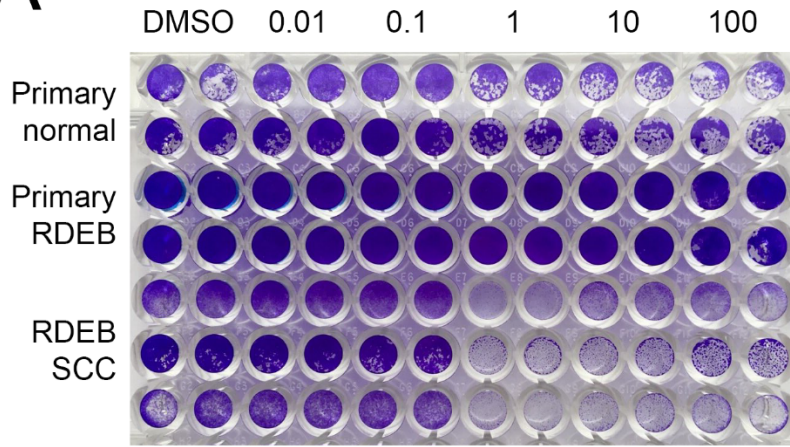
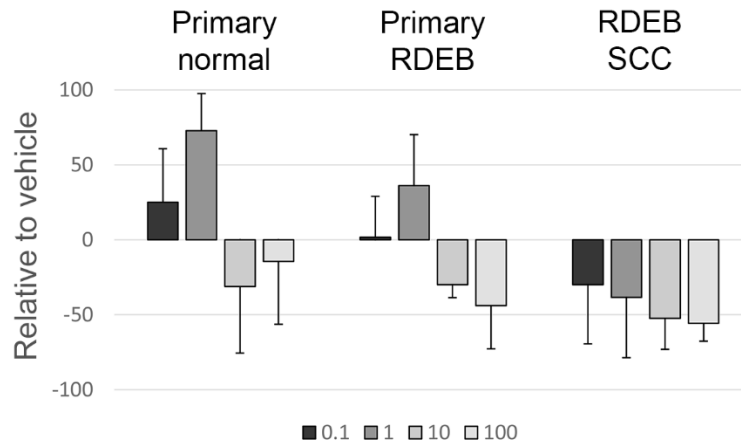
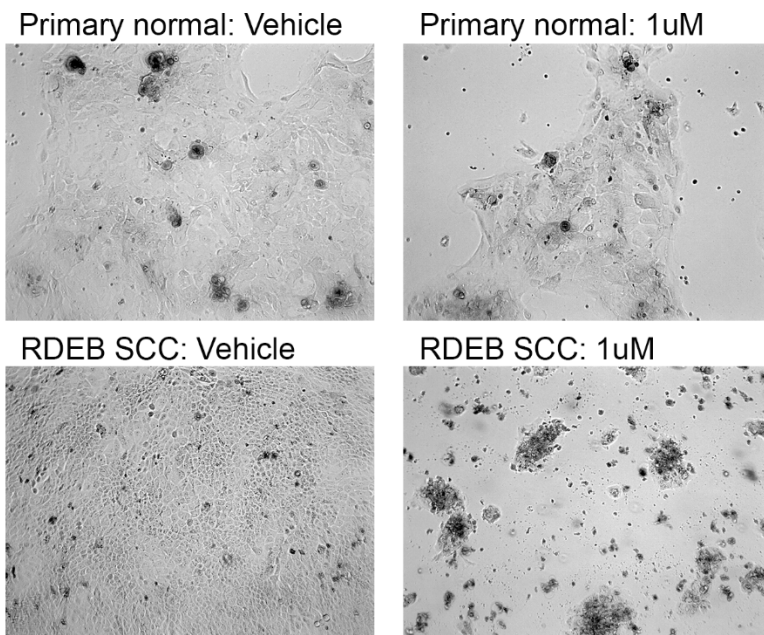
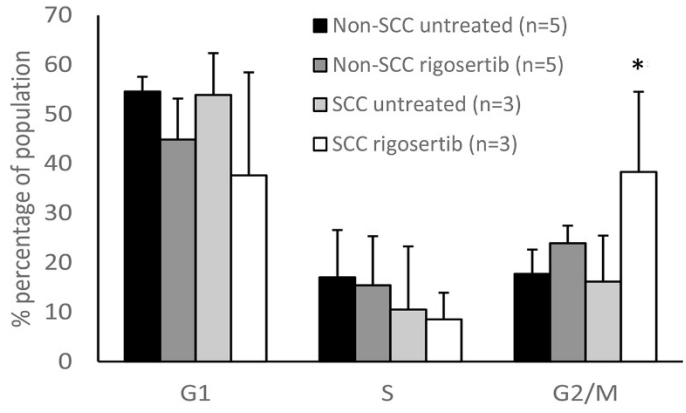
A**B****C**

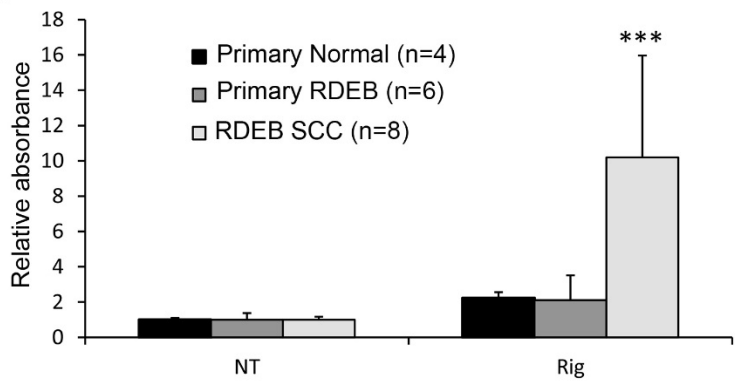
Figure 3: Rigosertib induces G2M arrest and apoptosis in RDEB SCC keratinocytes

A: Cell-cycle analysis in either RDEB SCC keratinocytes (SCCRDEB2, SCCRDEB3, SCCRDEB4, SCCCRDEB53, and SCCRDEB106) or non-SCC keratinocytes (Br61, RDEB115, RDEB124) treated with rigosertib (1uM, Non-SCC treated and SCC treated) or vehicle control (Non-SCC untreated and SCC untreated), and stained for BrdU and propidium iodide. Results expressed as percentage of cells at the G0/G1, S and G2/M phases of cell cycle 16 h following treatment. The results shown are the mean \pm s.d. **B:** Graph shows average absorbance increase using a colorimetric assay to detect cleaved nucleosomes in the cytoplasm as a measure of apoptosis after exposure of cells to vehicle or rigosertib. Data shown are the mean \pm s.d. are from two independent experiments using 2 populations of normal primary keratinocytes (Br46, Br61), 3 populations of primary RDEB keratinocytes (RDEB81, RDEB84, RDEB86) and 4 populations of RDEB SCC keratinocytes (SCCRDEB4, SCCRDEB53, SCCRDEB70, SCCRDEB106) exposed to 1uM of rigosertib for 16-24 hrs. **C:** Cells were cultured for 48 hrs in the presence (+) or absence (-) of 1uM rigosertib for 24 hrs and total cell lysates were prepared, transferred to nitrocellulose membranes and incubated with antibodies raised against phosphorylated CRAF (P-CRAF), total CRAF, phosphorylated AKT (P-AKT), total AKT and GAPDH. Samples loaded from left to right: Lanes 1-2 = normal primary breast keratinocytes (Br63), Lanes 3-4 = RDEB primary keratinocytes (RDEB84), Lanes 5-10 = RDEB SCC keratinocytes (SCCRDEB4, SCCRDEB62, SCCRDEB106). Graphs show data from two independent experiments. * = $p < 0.05$, *** = $p < 0.001$ (Student t-test).

A



B



C

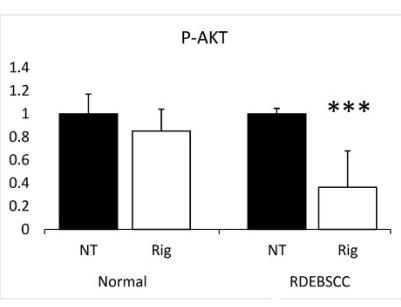
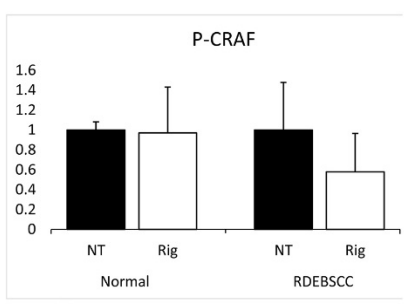
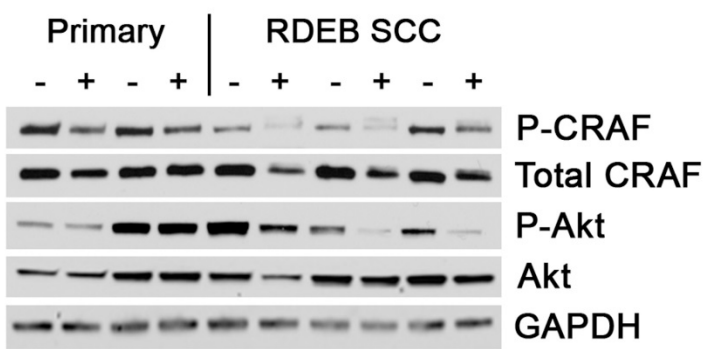
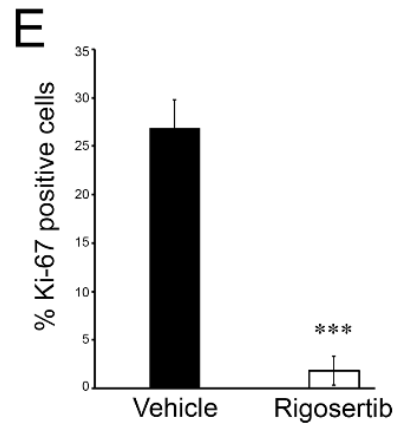
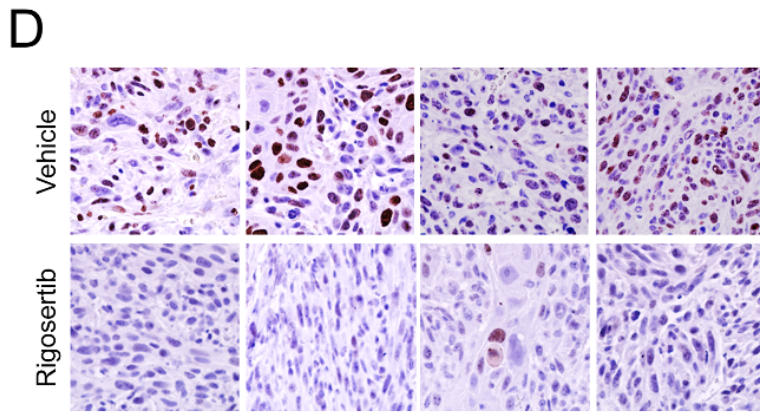
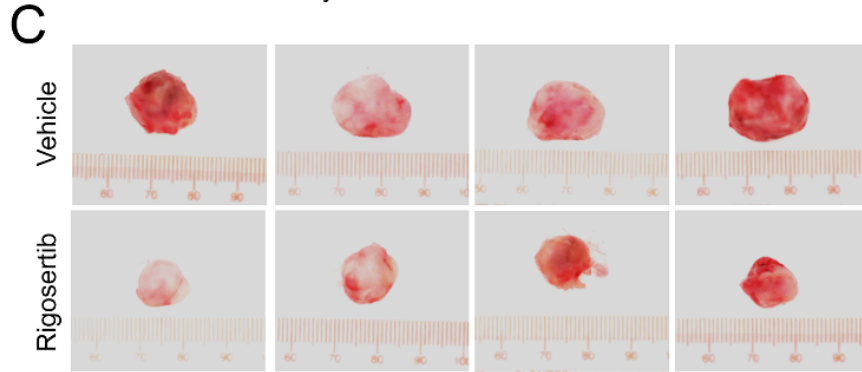
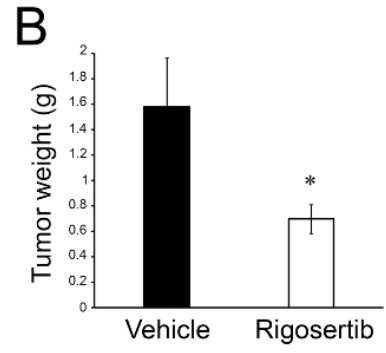
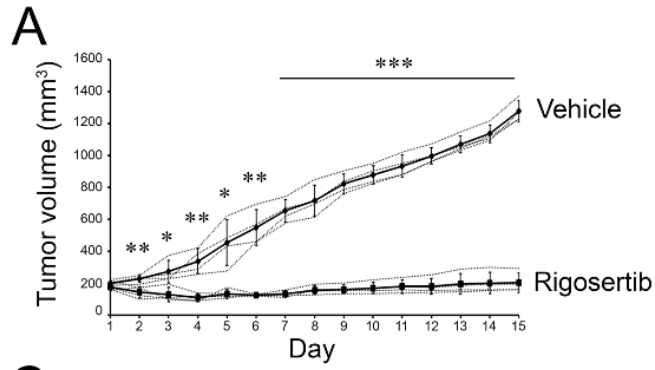


Figure 4: Rigosertib effectively targets RDEB SCC keratinocytes in vivo

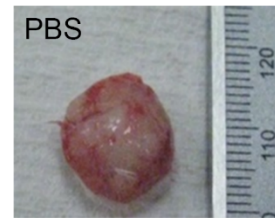
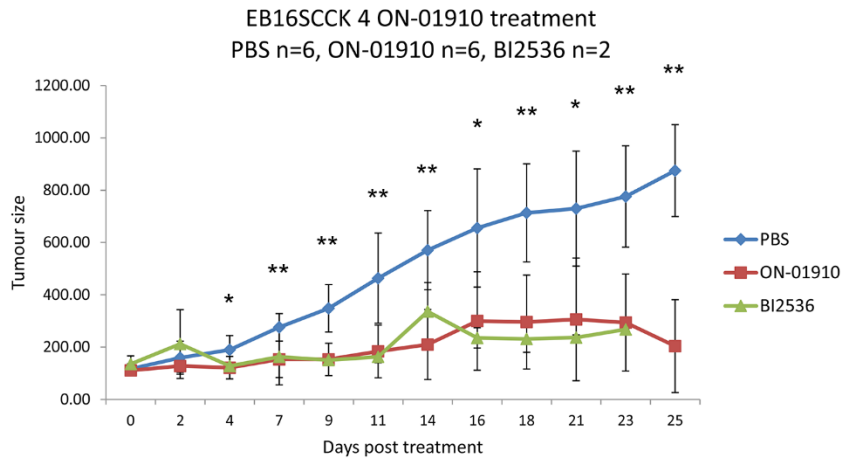
Animals bearing SCCRDEB106 xenograft tumors that had reached $>100\text{mm}^3$ were treated with either rigosertib (n=4) or vehicle control (n=4) injected IP every day for 14 days. Tumors were measured with calipers (**A**) until day 15 when animals were sacrificed, tumors were harvested, weighed (**B**) and photographed (**C**) before being bisected and frozen or fixed with formalin and paraffin embedded. **D**: 4uM FFPE sections were cut and incubated with an antibody recognizing Ki-67 (Abcam, ab16667, 1:200) as well as the nuclear stain hematoxylin. **E**: Graph shows the number of Ki-67 positive nuclei manually counted from five distinct microscopic fields for each tumor (n=8) at 20× magnification. * = $p < 0.05$, ** = $p < 0.01$, *** = $p < 0.001$ (Student t-test).



Supplementary Data

Supplementary Figure 1: Rigosertib effectively targets RDEB SCC keratinocytes in vivo

Animals bearing SCCRDEB16 xenograft tumors that had reached $\sim 100\text{mm}^3$ were treated with either rigosertib (n=6), vehicle control (n=6) or the PLK1 inhibitor BI-2536 (n=2) injected directly into the tumor every day for 6 days. Tumors were measured with calipers until day 25 when animals were sacrificed, tumors were harvested, and photographed. * = $p < 0.05$, ** = $p < 0.01$ (Student t-test).



References

1. Fine JD, Bruckner-Tuderman L, Eady RA, Bauer EA, Bauer JW, Has C, et al. Inherited epidermolysis bullosa: updated recommendations on diagnosis and classification. *J Am Acad Dermatol.* 2014;70(6):1103-26.
2. Fine JD, Johnson LB, Weiner M, Li KP, Suchindran C. Epidermolysis bullosa and the risk of life-threatening cancers: the National EB Registry experience, 1986-2006. *J Am Acad Dermatol.* 2009;60(2):203-11.
3. Mellerio JE, Robertson SJ, Bernardis C, Diem A, Fine JD, George R, et al. Management of cutaneous squamous cell carcinoma in patients with epidermolysis bullosa: best clinical practice guidelines. *Br J Dermatol.* 2016;174(1):56-67.
4. Christiano AM, Greenspan DS, Hoffman GG, Zhang X, Tamai Y, Lin AN, et al. A missense mutation in type VII collagen in two affected siblings with recessive dystrophic epidermolysis bullosa. *Nat Genet.* 1993;4(1):62-6.
5. Mellerio JE, Weiner M, Denyer JE, Pillay EI, Lucky AW, Bruckner A, et al. Medical management of epidermolysis bullosa: Proceedings of the 11nd International Symposium on Epidermolysis Bullosa, Santiago, Chile, 2005. *Int J Dermatol.* 2007;46(8):795-800.
6. Ng YZ, Pourreyron C, Salas-Alanis JC, Dayal JH, Cepeda-Valdes R, Yan W, et al. Fibroblast-derived dermal matrix drives development of aggressive cutaneous squamous cell carcinoma in patients with recessive dystrophic epidermolysis bullosa. *Cancer Res.* 2012;72(14):3522-34.
7. Mittapalli VR, Madl J, Loffek S, Kiritsi D, Kern JS, Romer W, et al. Injury-Driven Stiffening of the Dermis Expedites Skin Carcinoma Progression. *Cancer Res.* 2016;76(4):940-51.

8. Cho RJ, Alexandrov LB, den Breems NY, Atanasova VS, Farshchian M, Purdom E, et al. APOBEC mutation drives early-onset squamous cell carcinomas in recessive dystrophic epidermolysis bullosa. *Sci. Trans. Med.* 2018 *In press*
9. Purdie KJ, Pourreyaon C, Fassihi H, Cepeda-Valdes R, Frew JW, Volz A, et al. No evidence that human papillomavirus is responsible for the aggressive nature of recessive dystrophic epidermolysis bullosa-associated squamous cell carcinoma. *J Invest Dermatol.* 2010;130(12):2853-5.
10. Watt SA, Pourreyaon C, Purdie K, Hogan C, Cole CL, Foster N, et al. Integrative mRNA profiling comparing cultured primary cells with clinical samples reveals PLK1 and C20orf20 as therapeutic targets in cutaneous squamous cell carcinoma. *Oncogene.* 2011;30(46):4666-77.
11. Purdie KJ, Pourreyaon C, South AP. Isolation and culture of squamous cell carcinoma lines. *Methods Mol Biol.* 2011;731:151-9.
12. Chapman CM, Sun X, Roschewski M, Aue G, Farooqui M, Stennett L, et al. ON 01910.Na is selectively cytotoxic for chronic lymphocytic leukemia cells through a dual mechanism of action involving PI3K/AKT inhibition and induction of oxidative stress. *Clin Cancer Res.* 2012;18(7):1979-91.
13. Prasad A, Khudaynazar N, Tantravahi RV, Gillum AM, Hoffman BS. ON 01910.Na (rigosertib) inhibits PI3K/Akt pathway and activates oxidative stress signals in head and neck cancer cell lines. *Oncotarget.* 2016.
14. Prasad A, Park IW, Allen H, Zhang X, Reddy MV, Boominathan R, et al. Styryl sulfonyl compounds inhibit translation of cyclin D1 in mantle cell lymphoma cells. *Oncogene.* 2009;28(12):1518-28.

15. Athuluri-Divakar SK, Vasquez-Del Carpio R, Dutta K, Baker SJ, Cosenza SC, Basu I, et al. A Small Molecule RAS-Mimetic Disrupts RAS Association with Effector Proteins to Block Signaling. *Cell*. 2016;165(3):643-55.
16. Silverman LR, Greenberg P, Raza A, Olnes MJ, Holland JF, Reddy P, et al. Clinical activity and safety of the dual pathway inhibitor rigosertib for higher risk myelodysplastic syndromes following DNA methyltransferase inhibitor therapy. *Hematol Oncol*. 2015;33(2):57-66.
17. Anderson RT, Keysar SB, Bowles DW, Glogowska MJ, Astling DP, Morton JJ, et al. The dual pathway inhibitor rigosertib is effective in direct patient tumor xenografts of head and neck squamous cell carcinomas. *Mol Cancer Ther*. 2013;12(10):1994-2005.
18. Konieczkowski DJ¹, Johannessen CM², Garraway LA. A Convergence-Based Framework for Cancer Drug Resistance. *Cancer Cell*. 2018 33(5):801-815.